

27
6/18/79
26 7/17/79

SAND79-0813
UNLIMITED RELEASE

MASTER

DEVELOPMENT OF A 3 MV PULSE TRANSFORMER

G. J. ROHWEIN



Sandia Laboratories

TABLE OF CONTENTS

ABSTRACT	1
INTRODUCTION	1
SYSTEM DESCRIPTION	2
TRANSFORMER DESCRIPTION	6
OPERATIONAL RESULTS	11
CONCLUSIONS	15
ACKNOWLEDGEMENTS	15
REFERENCES	16

NOTICE
This document contains neither recommendations nor conclusions of the Federal Energy
Administration. It is the property of the Federal Energy Administration and is loaned to
your agency; it and its contents are not to be distributed outside your agency without
the express written permission of the Federal Energy Administration. It is to be
returned to the Federal Energy Administration when no longer needed.
FEDERAL ENERGY ADMINISTRATION
Washington, D.C. 20585

11

DEVELOPMENT OF A 3 MV PULSE TRANSFORMER*

by

G. J. Rohwein

Abstract

This report describes a 3 MV transformer designed for charging high voltage pulse forming transmission lines. The transformer is an air core spiral strip design which incorporates ring cage shielding to control edge breakdown in the secondary winding. The physical features of the transformer are described along with its electrical characteristics and the operational results.

Introduction

Air core transformers are an attractive alternative to Marx generators for charging high voltage pulse forming transmission lines (PFL) such as those used with high power electron or ion beam accelerators.^{1,2} Some of the advantages of transformer systems include simplicity, compactness, high reliability, reasonable cost and high energy transfer efficiency. The transformer described in this report was designed to demonstrate these features. The primary objective, however, was to establish the feasibility of multimegavolt operation. It was successfully tested to 2.2 MV in an off-resonance, single swing charging mode and to 3 MV in a dual-resonance charging mode. The energy transfer efficiencies for the two modes of operation were 58 and 91 percent, respectively. A 100 kV, 5 kJ capacitor bank was used to power the transformer for all experiments.

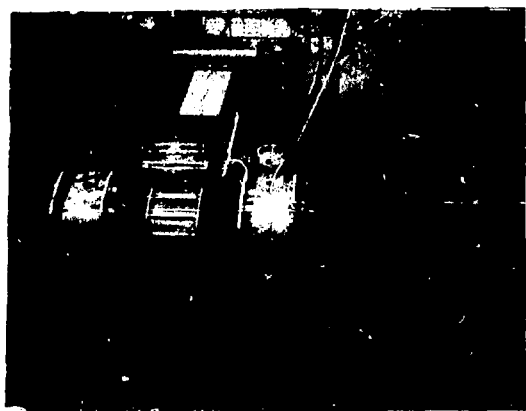
Spiral strip transformers are particularly well suited to PFL charging service because they inherently have a high interturn capacitance with a low total

capacitance to ground. This characteristic makes them much less vulnerable to dielectric breakdown between the final turns of the secondary winding from nanosecond voltage transients generated by discharges of the PFL than their helical wire wound counterparts. However, spiral strip windings are very susceptible to breakdown from the edges of winding strip unless special precautions are taken to prevent highly enhanced electric fields from occurring along these edges. This problem was avoided in the present transformer by placing concentric ring cages across the margins of the transformer which maintain a coaxial electric field distribution in these regions. The coaxial field across the margins is nearly parallel to the uniform field through the thickness of the winding and, as a result, the field enhancement along the edges is minimized. The ring cage, more fully described in the transformer section, does not have a measurable effect on the magnetic coupling of the transformer or contribute to eddy current losses. This type of ring cage shielding was used successfully on a number of earlier spiral strip transformers^{1,3,4} operated up to the 1 MV range and has proven to be effective on the present 3 MV model as well.

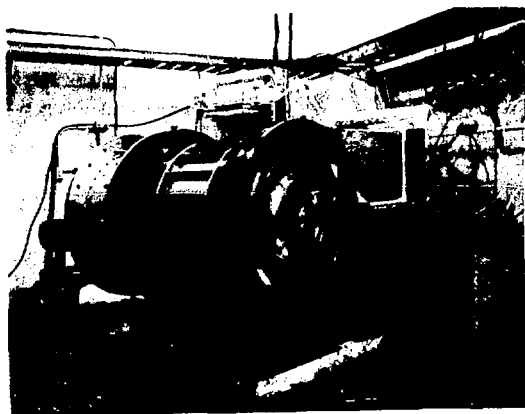
System Description

To test the transformer it was necessary to build a capacitor bank to provide primary pulsed power for the system. A load section was also required which included a capacitor, switch and load resistor. Two photographs of the system are shown in Fig. 1a and 1b. A cross sectional diagram is shown in Fig. 2.

The capacitor bank consisted of two 1.85 μ F capacitors arranged in an over-under configuration for charging to plus-minus 50 kV. The bank was electrically connected to the transformer primary through a parallel plate transmission line to minimize hookup inductance. A maximum output voltage of 100 kV was obtained by switching the capacitors in series with a spark gap placed between the high voltage



(a)



(b)

Fig. 1. a. 3 MV transformer test system.
b. Transformer and capacitor bank.

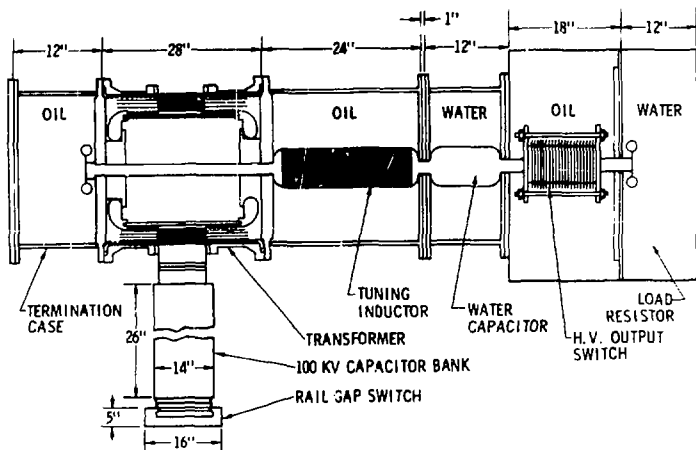


Fig. 2. Cross section of test assembly.

terminals of the capacitors. This switch was a commercially available rail gap and was triggered with a pulse generated by a 50 Ω coaxial cable typically charged to 70 kV. Triggered in this manner, and with an insulating gas mixture of 14.5 percent SF₆ and 85.5 percent Argon, the rail gap operated repeatedly in a multi-channel mode. Figure 3 is an electrical schematic of the system.

The load section, consisting of a coaxial water capacitor, a switch tank and a water load resistor, was connected in-line with the axis of the transformer. For the dual resonance tests an oil-immersed tuning inductor section was added between the transformer output and the water capacitor. The housings for both the capacitor and inductor were 60 cm diameter tube sections with acrylic interface plates between the oil and water sections. The switch and load resistor housings were open top box sections which permitted access to the interiors without

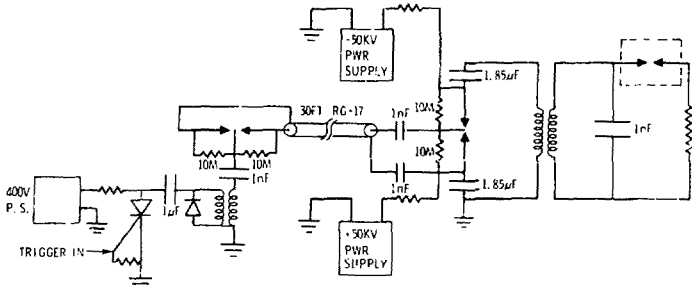


Fig. 3. Electrical schematic of transformer test system.

uncoupling the exterior assembly. The high voltage switch⁵ was a two-electrode, self-breaking gas-dielectric spark gap with disk grading rings in the housing (see Fig. 4). The self-break level could be varied over a range of 1 to 3 MV by controlling the SF₆ pressure in the switch.

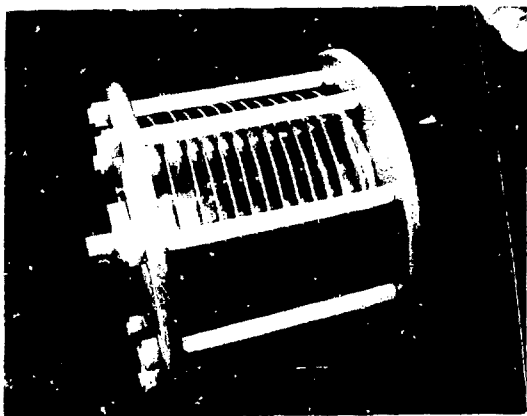


Fig. 4. Photo of P.V. spark gap.

Transformer Description

The transformer, shown in cross section in Fig. 5, has a single turn primary surrounding a 42-turn copper strip secondary winding. The active width of both windings is 30 cm. Eight layers of 0.019 cm thick polyester film provide the turn to turn insulation in the secondary which, with the .025 cm thick copper strip, make the finished winding thickness 7.6 cm. At 3 MV the mean winding stress is approximately 450 kV/cm. The width of the polyester insulation is 60 cm which leaves a 15 cm margin on both sides of the copper winding. The series of split concentric rings (Fig. 6) extending across both margins of the transformer are located on the core and case to provide electric field shaping outside the active winding area. The rings are spaced apart 0.32 cm to allow free passage of the magnetic field through the cage. Inside the case, the rings are potted in place with epoxy resin. Along the core, the rings are divided into four 90° arc segments and held in place by longitudinal bars attached to the core cylinder in the center of the winding and to a segmented torus at the outer ends of the core. The segmented torus is supported by an acrylic plate attached to the inside of the torus and by the 5 cm diameter copper output tube which extends through the assembly.

The field shaping provided by the ring cage is essential to prevent dielectric breakdown from the edges of the spiral winding. The concentric rings maintain a coaxial electric field distribution across the margins of the transformer which is nearly parallel to the uniform field through the thickness of the winding. The equipotential lines are thereby prevented from bending sharply around the edges of the thin winding conductor and creating highly enhanced electric fields. Figure 7 is a plot of the equipotential lines across one transformer margin, through an interface and into the water capacitor section.

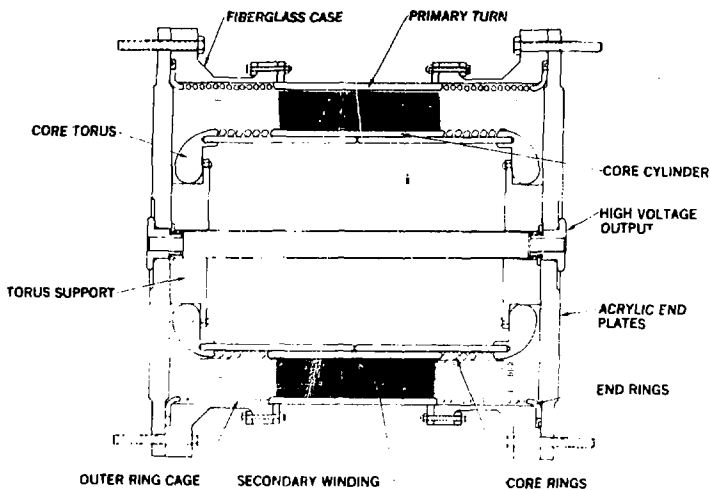


Fig. 5. 3 MV transformer.

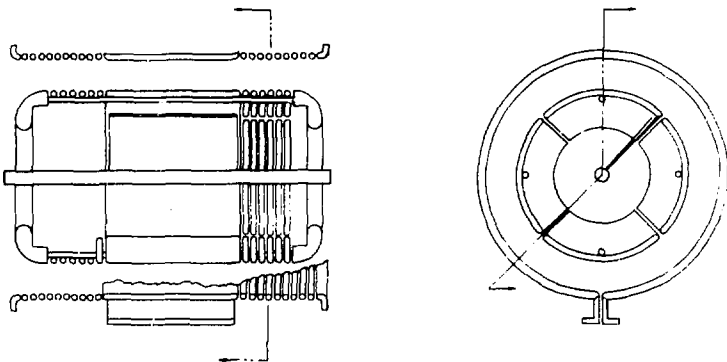


Fig. 6. Ring cage assembly.

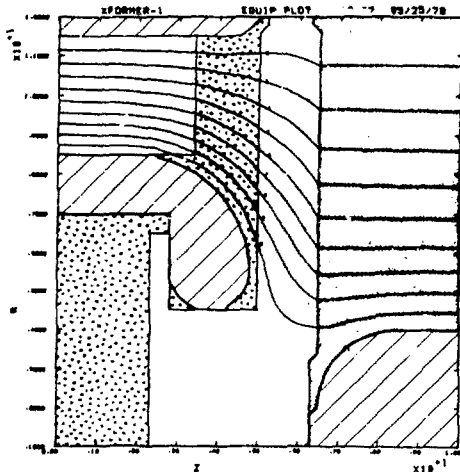


Fig. 7. Equipotential plot across one margin and the oil-water interface.

The rings on the core are divided into four symmetrical sections (Fig. 8) to prevent nanosecond voltage transients generated by the PFN discharge from breaking down the slots in the rings and core cylinder. This problem arises when the core diameter is large enough that the wave transit time around the circumference is a large fraction of or exceeds the shortest rise or fall time of the PFN voltage pulse (typically under 10 ns). Under these circumstances if the output of the secondary winding were connected along a line on one side of a single slot, a voltage equal to the full amplitude of the pulse could momentarily appear across the slot and cause a breakdown. This problem was studied in separate experiments where a fast rising voltage pulse (4 ns) was delivered to the ends of an array of full turn rings inside a simulated case. The rings consistently broke down across their gaps. The voltage pulse measured across the gap was equal to the full amplitude of the applied pulse for the duration of the ring transit time.

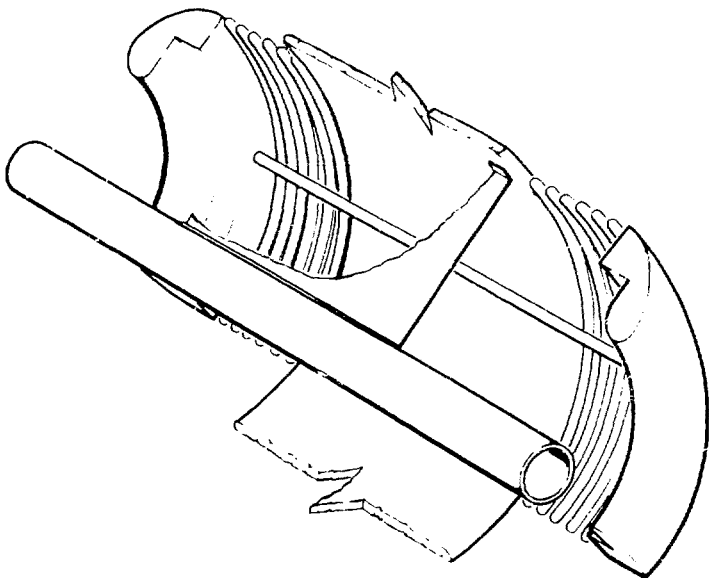


Fig. 8. One quadrant of core ring cage.

From these experiments it was found that gap breakdown could be eliminated by connecting the rings along a line opposite (180 degrees) the slot so that the voltage pulse swept symmetrically around the rings in opposite directions from the connection point. When the two fronts met at the gap, the voltage difference across it was essentially zero. The response time of the core ring cage was further shortened by dividing the rings into segments and separately connecting each set of segments to the center core cylinder along a longitudinal line through their mid sections. The output connection to the center cylinder, which is also the final turn of the secondary winding, was made opposite its slot to avoid similar transient voltage breakdown problems.

For structural reasons, the transformer case was made of two 60 cm diameter filament wound fiberglass reinforced polyester tube sections with integral flanges. The acrylic end plates are attached to these flanges which also provide a rigid connection to the external load system. The primary turn, located between the fiberglass case sections, is also part of the structural assembly. It is attached to the fiberglass sections with shallow flanges around each edge of the turn. This arrangement facilitates assembly of the transformer and, when used in repetitive pulse service, eases the problem of heat removal from the primary turn. The fiberglass case sections are longitudinally slotted and aligned with the slot in the primary turn to provide space for feeding the insulation sheets through the side of the assembly. The slot and sheets are sealed with silicone rubber adhesive to prevent oil leakage from the interior of the transformer.

When the physical assembly was complete the transformer was placed in a vacuum chamber for oil impregnation. The oil used was an oxidation inhibited water white mineral oil. It was held under vacuum continuously for three weeks to assure full oil penetration through the secondary winding and removal of all absorbed gasses and moisture. After completing the impregnation cycle the transformer was ready for testing.

The measured and calculated electrical parameters of the transformer are as follows:

Primary inductance, L_p = .590 μ H
Secondary inductance, L_s = 488 μ H
Mutual inductance, M = 14 μ H
Coupling coefficient, K = .83

These values were calculated using Nagaoka's inductances formulas⁵ and later verified by measurements.

$$L_p = .004\pi a \left[\ln \frac{8a}{b} - \frac{1}{2} \right] \mu\text{H}$$

$$L_6 = .0197 \left(\frac{2a}{b}\right) N^2 abk' \quad \mu\text{H}$$

$$M = .004\pi^2 a^2 n_1 n_2 [r_1 B_1 - AB_2] \quad \mu\text{H} \text{ (for coils of the same axial length)}$$

where

a and b are the mean radius and axial length of the coil, respectively.

N is the total number of turns.

n_1 and n_2 are the turn densities per centimeter length for the primary and secondary windings.

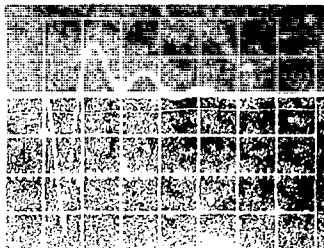
k and k' are functions of $b/2a$ taken from tables.

r_1 is the diagonal distance from the inside radius of one edge of the primary turn to the smallest inside radius of the secondary winding at the opposite edge.

B_1 and B_2 are functions of the ratio of the mean coil radii and are taken from tables.

Operational Results

Initially the transformer was operated in an off-resonance single swing charging mode. For these tests the capacitor bank was coupled directly to the transformer primary turn and the transformer output fed directly to the 1.1 nF load capacitor. Under these conditions the charge time on the load capacitor was 1 μs . A typical waveform for the single swing charging tests is shown in Fig. 9. The system was tested at successively higher voltages until at 1.8 MV a breakdown occurred between one core torus and the outer ring cage. The breakdown flashed across one of three acrylic spacer blocks which had been placed between the acrylic end plate and the winding insulation to prevent lateral displacement of the winding. Only the acrylic block was damaged. The transformer was drained and all three blocks on that side were removed. After refilling the transformer with oil, testing was resumed and the system was taken to a maximum of 2.2 MV without further



12

Figure 12 shows a 4x4 grid of 16 small grayscale images, likely a test pattern or calibration chart, used for image processing or quality control. The images are arranged in a 4x4 matrix. The first three rows contain four images each, and the fourth row contains only three images. The images show various patterns of black and white dots and lines, including a central crosshair and a grid-like structure. The images are slightly noisy and have different contrast levels, suggesting they are different frames or different parts of a single frame. The overall layout is a standard calibration grid used in optical microscopy or similar imaging applications to ensure the quality and alignment of the images.

one sets. Figure 13 shows the results.



Fig. 10. Dual resonance charge cycle voltage.
Sweep = 1 μ s/div. Voltage = 1.1 MV/div.

time on the side opposite the previous breakdown where the acrylic spacer blocks had not been removed. The arc flashed across one of the remaining acrylic spacers in a manner similar to the first breakdown. To repair the transformer it was drained, opened and the remaining blocks removed. The damage was again minimal. The arc had tracked radically across the extreme edges of the polyester insulation between the sheets and the block. The winding was repaired by trimming back the insulation to just below the depth of the arc path, approximately 1 mm.

Since the spacer blocks had originally been installed to prevent the central layers of the winding from shifting when the transformer was handled with its axis in a vertical position, it was necessary to devise some other method to hold the winding in place. This was accomplished by fusing the edges of the insulation sheets together along a number of radial lines around the edge of the winding. A heated soldering iron was used for this operation. The flat tip was drawn across the edge of winding which melted the polyester film locally and fused the adjacent sheets together. The depth of the fused lines was approximately 3 mm. With eight such lines the winding was held securely from slipping and yet the oil could flow freely into the winding when the unit was impregnated.

When the transformer was repaired and reimpregnated, testing was resumed. No further transformer breakdowns were experienced up to and including the 3 MV level.

This corresponded to a ± 45 kV charge on the primary capacitor and an energy transfer efficiency of 91 percent. A number of breakdowns did occur, however, in the water capacitor and in the switch tank between 2.5 and 3 MV which precluded the possibility of taking the system above 3 MV.

Conclusions

The present experiments with the 3 MV transformer clearly demonstrate the feasibility of multi-megavolt transformer operation for pulse charging applications. The key to obtaining reliable performance with spiral strip transformers lies in proper electric field shaping in the margins of the transformer. This can be achieved by placing concentric split ring caps across the margins which confine the electric field to a coaxial distribution but does not disrupt the magnetic coupling. This technique of field shaping, used successfully on earlier transformers operated in the one megavolt range, has proven to be an effective method for multi-megavolt operation also.

Having demonstrated that spiral strip type transformers can operate reliably up to at least 3 MV, another option is available in designing pulse charging systems for high voltage accelerators and other fast pulse discharge devices. Transformer powered systems have the general appeal of high efficiency, simplicity, compactness and comparatively low cost. In cases where these features are important, therefore, transformer systems can be employed advantageously.

Acknowledgements

The author wishes to thank E. R. Prestwich for his encouragement and valuable suggestions and E. L. Sean for his field calculations. The assistance of J. P. Corley, M. W. O'Malley and R. W. Larson in the assembly, setup and testing of the transformer is also gratefully acknowledged.

References

1. G. J. Rohwein, TRACE I, A Transformer Charged Electron Beam Generator, IEEE Transactions on Nucl. Sci., Vol. NS-22, No. 3, June 1975.
2. A. P. Avrorov, V. T. Astrelin, E. L. Bogarinsev, V. A. Kapitonov and V. M. Lagunov, A Pulsed Electron Beam Accelerator, AQUACEN, Proc. of the Int'l. Pulsed Power Conf., Lubbock, TX, IEEE11, 1976.
3. G. J. Rohwein, M. T. Buttram and K. R. Prestwich, Design and Development of a 350 kV, 100 pps Electron Beam Accelerator, 2nd Int'l. Topical Conf. on High Power Electron and Ion Beam Res. and Tech., Vol. II, October 1977.
4. High Voltage Transformer Development, Electron Beam Fusion Progress Report, April 1977 through Sept. 1977, SAND78-0080.
5. J. J. Ramirez, Private Communication, High Voltage Switch Designed by Ramirez for two to three megavolt operation.
6. F. W. Grover, Inductance Calculations, Dover Publications, Inc., 1946.
7. D. Finkelstein, P. Goldberg and J. Shuchatwitz, High Voltage Impulse System, Review of Sci. Instr., Vol. 37, No. 2, Feb. 1966.
8. E. A. Abramyan, Transformer Type Accelerators for Intense Electron Beams, IEEE Trans. on Nuclear Science, Vol. NS-18, No. 3, June 1971.

DISTRIBUTION

Los Alamos Scientific Laboratory
P. O. Box 1663
Los Alamos, NM 87544

Attn: J. Sargent
P. Mace, AP-2
G. Erickson, AP-1
Y. Jansen, L-7
K. Riepe, L-7
T. Stratton, L-7
C. Fowler, M-6
G. Frank, L-5

Lawrence Livermore Laboratory
P. O. Box 808
Livermore, CA 94550
Attn: E. Cook (!)
L. Reginado

Physics International Co.
2700 Merced St.
San Leandro, CA 94577
Attn: B. Bernstein
T. Naff
P. Champney
A. Toepfer

Ion Physics Corp.
P. O. Box 416
Burlington, MA 01803
Attn: H. Milde

Dept. of Energy
Office of Inertial Fusion
Washington, DC 20545
Attn: P. Hoff
T. Godlove
E. Braunsweig
G. Canavan

Atomic Weapons Research Establishment
Aldermaston, Berk., England
Attn: J. C. Martin, SSWA-H36

Maxwell Laboratories
9244 Balboa Ave.
San Diego, CA 92123
Attn: A. C. Kolb

Defense Nuclear Agency
Washington, DC 20305
Attn: G. Soper

System, Science and Software
P. O. Box 4803
Hayward, CA 94540
Attn: A. Klien
G. Loda
H. Aslin

Air Force Weapons Lab
Kirtland AFB
Albuquerque, NM 87117
Attn: D. Straw
C. Clark
A. Guenther
P. Ortwerth
W. Baker

Naval Research Laboratory
Code 7720
Washington, DC 20375
Attn: J. Shipman
I. Vitkovisky

Ian Smith, Inc.
3115 Gibbons Dr.
Alameda, CA 94501
Attn: I. Smith

Energy Sciences Inc.
111 Terrace Hall Ave.
Burlington, MA 01803
Attn: S. Nablo
S. Denholm

Naval Surface Weapons Center
White Oak Laboratory
Silver Spring, MD 20910
Attn: F. Rose

Aerospace Corp.
2350 East El Segundo Blvd.
El Segundo, CA
Attn: R. Hofland

Pulsar Associates, Inc.
11491 Sorrento Valley Rd.
San Diego, CA 92121
Attn: W. Grewson

U.S. Army Ballistic Research Lab
Aberdeen Proving Ground, MD 21005
Attn: D. Eccleshall

Westinghouse Electric Corp.

Research & Development

P. O. Box 10864

Pittsburg, PA 15236

Attn: W. Bratkowski

4254 S. A. Goldstein

8266 E. A. Aas (1)

3141 T. L. Werner (5)

3151 W. L. Garner (3)

DOE/TIC (25)

(R. P. Campbell, 3172-3)

Simulation Physics

41 "B"Street

Burlington, MA 01803

Attn: R. Little

Harry Diamond Laboratory

Branch 230

2800 Powder Mill Rd.

Delphi, MD 20783

Attn: A. Kehs

400 J. A. Mogiord

4000 A. Narath

4200 G. Yonas

4210 J. B. Gerndo

4216 R. A. Gerber

4230 W. Cowan

4232 W. Beezhold

4232 C. MacCallum

4232 P. E. Bolduc

4240 G. W. Kuswa

4244 P. A. Miller

4244 D. J. Johnson

4244 S. Humphries

4244 C. W. Mendel

4250 T. H. Martin

4251 G. W. Barr

4251 R. A. White

4251 T. Franklin

4251 I. D. Hamilton

4252 J. P. VanDevender

4252 D. L. Johnson

4252 D. H. McDaniel

4252 E. L. Neau

4252 R. S. Clark

4253 K. R. Prestwich (10)

4253 D. L. Cook

4253 M. T. Buttram

4253 J. P. Corley

4253 M. W. O'Malley

4253 A. W. Sharpe

4253 R. B. Miller

4253 J. J. Ramirez

4253 W. K. Tucker

4253 G. J. Rohweln (10)

4253 J. H. Snethen

4253 L. E. Stevenson